ChemComm

Accepted Manuscript

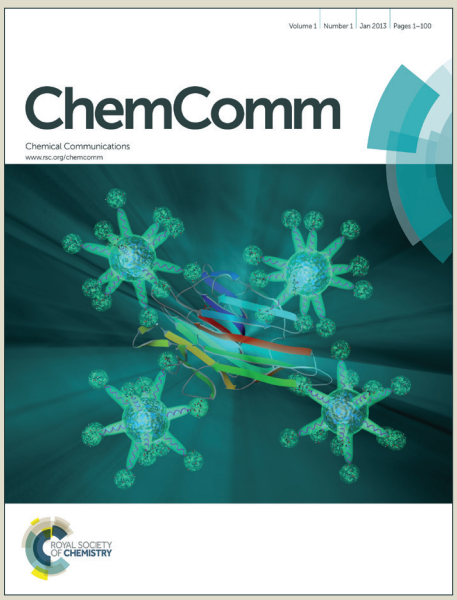

ROYAL SOCIETY OF CHEMISTRY

www.rsc.org/chemcomm

Journal Name

RSCPublishing

COMMUNICATION

Layer-by-layer assembly of a redox enzyme displayed on the surface of an elongated bacteria into a hierarchical artificial biofilm based anode

Cite this: DOI: 10.1039/x0xx00000x

Received 00th January 2012,
Accepted 00th January 2012

DOI: 10.1039/x0xx00000x

www.rsc.org/

Lin Xia[a,b], Yehonatan Ravenna[a] and Lital Alfonta[*a]

To achieve an efficient electron transfer communication between bacteria and electrode，several strategies including enzyme surface display, bacteria elongation as well as layer-by-layer techniques were used to assemble bacteria, methylene blue, multiwall carbon nanotubes, and carbon papers into a hierarchical micro/nano artificial biofilm based bioanodes.

Microbial fuel cells (MFCs) convert chemical energy of organic matter into electrical energy by utilizing the metabolism of an entire living microorganism,[1,2]. This is a novel approach to creating self-sustaining systems that can effectively convert organic matter and renewable biomass into electricity[3-5]. Although MFCs already show promising applications including energy recovery from waste water treatment[6] marine sediment[7], and environmental monitoring power device,[8] long-range electron transfer pathways as well as poor communication between microbe and electrodes impair the energy conversion efficiency. In enzymatic biofuel cells, purified enzymes are used as catalysts to achieve energy conversion.[9] Compared with microbial fuel-cells, its catalytic efficiency is higher due to an improved electron transfer pathway between enzymes and electrodes, as well as higher surface density of the biocatalysts. However, the extra cost and labour involved in enzyme expression and purification and the inevitable loss of enzyme activity during long-term operation are two prominent disadvantages that have limited its practical use.

Microbial surface display exhibits several advantages in bioelectrochemical systems including shorter electron transfer pathways by the expression of highly active redox enzymes on the cell surface and elimination of the laborious and expensive enzyme purification step. The strategy of bacterial surface expression of redox enzymes is an ideal method to overcome the above-mentioned disadvantages existing in microbial and enzymatic fuel cells. Moreover, this technology enables us to expand the MFCs application areas with more choices of microorganism species other than exo-electrogens, consequently expanding the fuel range. Recently, this strategy has been demonstrated in the applications of yeast based MFCs[10, 11] and *E. coli* based biofuel cells (BFCs) [12, 13] using different biofuels.

Another important influence on the bacteria-electrode communication is the formation of a biofilm, a structured microbial community adhere to the MFC's anode and plays a key role in extracellular electron transfer[14]. Biofilm can facilitate an efficient bacterial electron transfer in MFCs primarily due to much higher biomass densities and higher bacterial viability stemming from anode respiration.[14-16] However, natural anodic biofilms usually suffer from diffusion and mass transfer limitations as well as insufficient interaction of bacteria with anode materials, which impede the electron flow between the microbe surface and an electrode.[17] Therefore, optimizing the inner structure and thickness of the anodic biofilm may prove a successful strategy to enhance MFCs performance.

From electrode material considerations; anode modification with nano-materials including conducting polymers[18], carbon nanotubes [19]and metal oxides[20] has been proposed to promote anodic biofilm formation as well as to better the interaction between microbes and electrodes. However, random formation of natural biofilm on the nano-modified electrode surface as well as the variation in thickness and lack of communication between electrodes and the actual catalytic site still limit the advantage of these nanomaterials which were previously used for purified enzyme systems.[21,22]

Here, we present a novel hierarchical bioanode assembly taking both microbial and electrode material aspects into consideration. To achieve a highly efficient electron transfer communication between bacteria and electrode, bacteria were genetically engineered to have surface-displayed ADHII,[12] and then treated with cis-diammineplatinum (II) dichloride (cisplatin) for filamentous growth. Layer-by-layer (LbL) technique was used to assemble bacteria, mediatorsmultiwalled carbon nanotubes (MWCNTs), and carbon papers into a hierarchical mircro/nano artificial biofilm based bioanode (Scheme 1).

To increase interaction of bacteria with the modified electrode on the individual bacterium level, changing the shape and size of the microorganism could be an effective approach in assisting the electrode nano-modification endeavour. Specifically, for ellipsoidal shaped or rod shaped bacteria like *E. Coli,* increase in aspect ratio may transform them into more twisted, longer threadlike shape that may render them more inextricably intertwined with the micro/nano materials on the electrode support. For this purpose, an approach initially reported by Rosenberg et al.[23,24] demonstrated that adding platinum salt to bacterial growth media has driven bacteria in the direction of filament growth. Recently, similar strategy has also been demonstrated in *S. oneidensis* based MFCs.[25] We assumed that this

approach could prove promising for our ADHII surface displaying *E. coli*.

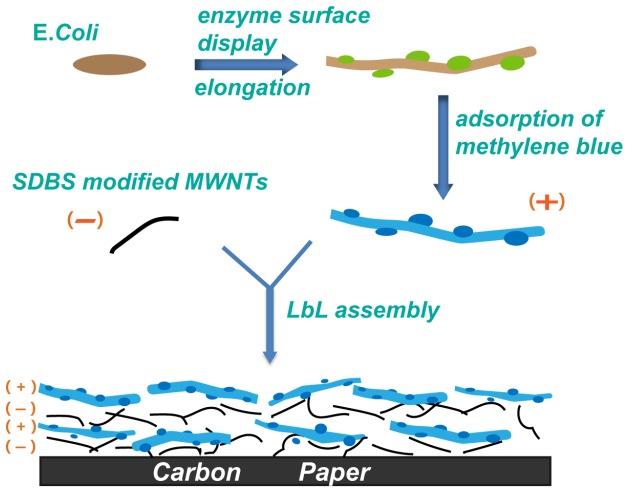

Scheme 1. Schematic presentation of LbL assembly and elongated E. coli surface displaying an enzyme, into a hierarchical artificial biofilm based anode.

Although previous research has shown that platinum salt induced filamentous growth of *E. coli*,[23,24] the effects of platinum salt on *E. coli* with auto-display system (JK321 strain harbouring plasmid pJM7) has not been evaluated yet. Therefore, the influence of the cisplatin on the growth rates and the activity of ADHII surface-displayed on *E. coli* (ADHII-JK321) have been investigated first. Fig.1A shows growth curves of bacteria grown in the presence of different concentrations of cisplatin. Compared with the growth curve of untreated ADHII-JK321 (black), there is only a slight decrease in the growth rate after 8 hours of growth (red and green) when treated with moderate amounts of cisplatin (10-25 µg/mL). This may suggest that the presence of moderate amounts of cisplatin do not inhibit significantly cell division in the log phase of bacterial growth. However, when the concentration of cisplatin increase to a toxic level (50µg/mL), the inhibition effect on bacteria growth becomes dominant in almost all growth phases (blue). Following growth rate measurements, the influence of cisplatin treatment on surface displayed ADHII activity was investigated as shown in Fig. 1B. Interestingly, the highest activity was attained from the sample treated with 15 µg/mL cisplatin, which presented ca. 50% higher activity than that of the untreated ADHII-JK321. The sample grown in the presence of 50 µg/mL cisplatin showed significant loss in enzyme activity probably due to cisplatin toxicity.

To understand the origin of ADHII activity increase after a moderate amount of cisplatin treatment, enzyme activity was investigated by comparing the ADHII activity assay of commercial ADHII in the presence and absence of 15µg/mL cisplatin in the activity medium. Results (shown in Fig. S1A, ESI) suggest that cisplatin effect on purified ADHII activity is negligible. Next, comparing the ADHII activity assay of wild type *E. coli* strain JK321 (WT) (not displaying ADHII) grown in the presence or absence of 15µg/mL cisplatin tested the possibility that the presence of cisplatin could induce cell stress response. Both samples of WT bacteria before and after cisplatin treatment have shown very low basal ADHII activity (Fig. S1B, ESI).

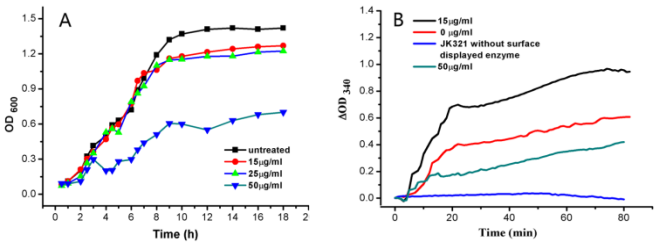

Fig. 1 Growth curves (A) and ADHII enzyme activity assay (B) of cisplatin treated ADHII-JK321 *E. coli*.

We thus hypothesized that the increase in ADHII activity of ADHII-JK321 after cisplatin treatment may be attributed to the increased amount of surface-displayed enzyme along with bacterial elongation. Through statistical data obtained by a cell counter, the average length of the untreated ADHII-JK321 was estimated to be 1.2µm (verified by SEM images as well). The number of bacterial cells in solution (when O.D.=1.0) was estimated to be 8.9×10^7 cells per mL, while for elongated bacteria the average length was measured to be 6.4µm and 1.0 O.D. was calculated as representing only 2.6×10^7 cells per mL. These results show that there are much less bacterial cells in the cisplatin treated samples due to the presence of mostly non-dividing bacteria than in the untreated bacterial cells. Combining the result from activity measurements of surface displayed ADHII we could estimate ca. 12,000 active enzyme copies per untreated ADHII-JK321 cell whereas the activity measurements of the surface displayed ADHII on treated bacteria resulted in ca. 61,000 active enzyme copies per cell (calculated according to curve in Fig. S2, ESI). If we calculate these results and normalize it to enzyme copies per length (µm) of bacteria, untreated bacteria display roughly the same enzyme copy number per µm as the cisplatin treated bacteria (ca. 10,000 copies). Therefore, the increase in ADHII activity of elongated ADHII-JK321 may be attributed both to elongation which enables more enzyme copies per bacteriumin addition to more enzyme copies for the same O.D. of bacterial growth media.

SEM imaging was used for the study of the structure and morphology of the bioanode. Representative images of different modified carbon paper electrodes (CPE) are given in Fig. 2. Fig. 2A, shows bare CPE which is poorly covered with elongated bacteria. This suggests that interaction between bacteria and carbon paper needs to be further improved to achieve better surface coverage. Even after longer incubation time of ca. 18 hours of the bare CPE in the bacterial growth medium, biofilm formation is still random and unevenly distributed on the CPE (Fig. 2A, inset). To improve bacteria-electrode interactions, LbL assembly was employed to create an artificial on the CPE surface. Prior to the LbL assembly, two oppositely charged layers were prepared. The negatively charged layer was made of sodium dodecyl benzene sulfonate (SDBS) modified MWCNTs, whereas the elongated ADHII-JK321 adsorbed with MB has served as a positively charged layer. There were two reasons for us using MB adsorption on bacterial surface instead of on MWCNTs surface. First, once MB molecules adsorbed on carbon surface via π-π stacking interactions, their molecular structure has changed[26] and lost the ability to mediate NADH oxidation in a desirable low potential suitable for a bioanode MFC (i.e. at least below -0.1V vs. Ag/AgCl, Fig. S3, ESI). Second, adsorption of MB on bacterial surface occurs through electrostatic interactions due to a negatively charged bacterial surface in neutral pH. This interaction did not compromise the electron transfer mediation ability of MB towards NADH oxidation,

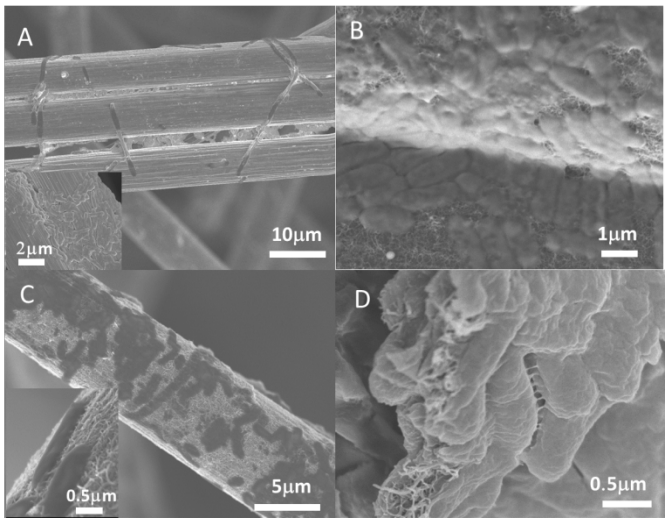

Fig. 2 SEM images of different modified CPE anodes, (A) bare CPE covered with elongated ADHII-JK321. Inset: natural biofilm of ADHII-JK321, (B) one bilayer of LbL assembled ADHII-JK321/MB/MWCNTs/CPE, (C) one bilayer of LbL assembled elongated ADHII-JK321/MB/MWCNTs/CPE, inset: tilted view of elongated bacteria on MWCNTS/CPE, (D) a cross-section view of the LbL assembled elongated ADHII-JK321/MB/MWCNTs/CPE with 5 bilayers illustrating the inter-layer contact.

which was further verified by electrochemical characterization. Besides, another advantage of using MB molecules to assist the LbL assembly is that the electron transfer pathway between bacteria and electrode rendered much shorter. It is shown in Fig. 2B and C that the surface coverage of CPE by bacteria is significantly improved after only one layer of LbL assembly. It could also be estimated from Fig. 2A and 2C that the length of the elongated bacteria could reach more than 20μm in some cases. Moreover, the contact area of elongated bacteria coiled on the MWCNTs modified carbon fibre (the basic components of CPE) via electro-static assembly has greatly increased (Fig. 2C). Fig. 2D shows a cross section view of the LbL assembled elongated ADHII-JK321/MB/MWCNTs/CPE after 5 repeats. The detailed view demonstrates a network of MWCNTs connecting between monolayers of elongated bacteria. This network functions as an artificial biofilm suitable for electron transfer.

To evaluate the bacteria-electrode communication of the LbL assembled artificial biofilm, cyclic voltammetry (CV) was used. CV results of the catalytic performance of different electrodes towards ethanol oxidation are shown in Fig. 3. As ADHII is an NAD^+ dependent enzyme, evolution of anodic bioelectrocatalytic current resulting from the enzymatic oxidation of ethanol was clearly visible and is directly related to the oxidation of NADH that was mediated by MB molecules. As expected, the best performance was observed from the LbL assembled bioanode (elongated ADHII-JK321/MB/MWCNTs/CPE) with 5 layers of assembly (Fig. 3A). As a comparison, LbL assembled anode with untreated bacteria show about half of the catalytic current and a much smaller current change upon addition of ethanol (Fig. 3B). This difference suggests that not only does the cisplatin treated ADHII-JK321 more enzymatically active, but it also indicates that the bacteria-electrode communication in the artificial biofilm with elongated bacteria is improved. Fig. 3C shows the anodic catalytic performance of a bioanode constructed from a natural biofilm of ADHII-JK321 formed on CPE surface but MB in solution. The anodic catalytic current attained was less than 20% of the artificial LbL biofilm with elongated bacteria. Besides, there was a slight negative shift with the oxidation peak of the natural biofilm modified electrode, which may be attributed to local pH changes inside the biofilm. At the same time, the oxidation peak of MB shows no shift in case of the LbL assembled artificial biofilm, which suggests an improved diffusion and mass transport within the local electrode environment. Fig. 3D shows a plot of a catalytic peak current change upon addition of 1.5% ethanol plotted against the number of assembled bilayers, which suggests that the anode that consists of 5 bilayers of bacteria and MWCNTs shows the best catalytic performance.

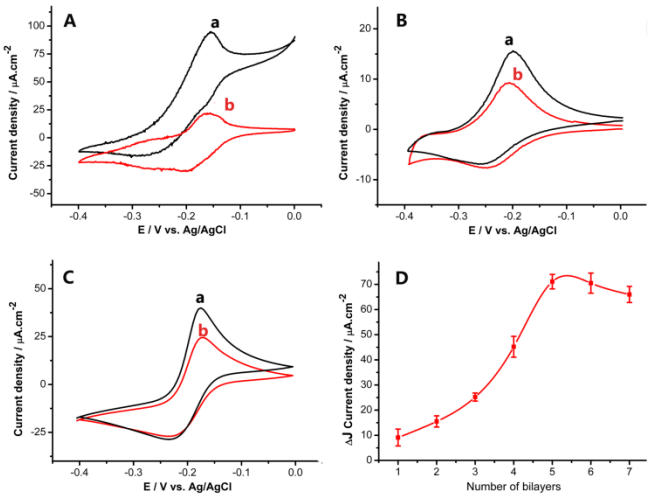

Fig. 3 Cyclic voltammograms of different CPE anodes demonstrating bioelectrocatalytic ethanol oxidation (A) Elongated pJM7-ADHII JK321/MB/MWCNTs/CPE with 5 layers of LbL assembly; (B) Untreated pJM7-ADHII JK321/MB/MWCNTs/CPE anode with 5 layers of LbL assembly; (C) natural biofilm of pJM7-ADHII JK321 modified on CPE with with (a) and without (b) 1.5% (wt) ethanol; (D) catalytic current dependence (oxidation peak current evolution upon addition of ethanol) plotted against the number of bilayers assembled for elongated pJM7-ADHII JK321/MB/MWCNTs/CPE. Spline interpolation was applied to fit the data. Scan rate: 5 mV/s in PBS buffer (pH7.4) in the presence of 5mM NAD^+ and 1.5% ethanol, all potentials are reported vs. Ag/AgCl.

Subsequently, BFCs were assembled based on differently modified CPE anodes. The cathode was controlled by a potentiostat similarly to the way it was described by Schröder et al.[27] and was biased continuously at +700 mV vs Ag/AgCl electrode. The fuel at the anode was ethanol, and the fuel cell was of one compartment configuration and was exposed to an ambient atmosphere. The performance of the biofuel cell with different anodes is shown in Fig.4. Fig.4A shows the power output from the modified bioanodes based BFCs. The best performance was achieved by the BFCs with elongated ADHII-JK321/MB/MWCNTs/CPE anode composed of 5 bilayers of LbL assembly, with a maximum power output of 70.6μW/cm^2 (curve a). The LbL assembled anode with untreated ADHII-JK321 has shown a lower power output of 43.5μW/cm^2 (curve b). Natural biofilm covered CPE anode had a minimal power output of 10.7 μW/cm^2 (curve c). As a control experiment, commercial ADHII from yeast was electrostatically assembled on MWCNTs modified CPE to serve as an anode in BFC. The ADHII solution concentration was adjusted to be similar to estimated active enzyme units as the activity measured for the surface displayed ADHII. The maximal power output was 22 μW/cm^2 (curve d). From comparison of polarization curves shown in Fig. 4B, the BFCs with elongated ADHII-JK321/MB/MWCNTs/CPE anode demonstrated a polarization curve closer to rectangular shape, which is the ideal voltage–current relationship for an electrochemical generator of electricity. The fill factor (*f*) of the biofuel cell was ca. 37%, calculated according to equation (1). Where P_{max} is the maximum

power output, I_{sc} is the short-circuit current and V_{oc} is the open circuit voltage.

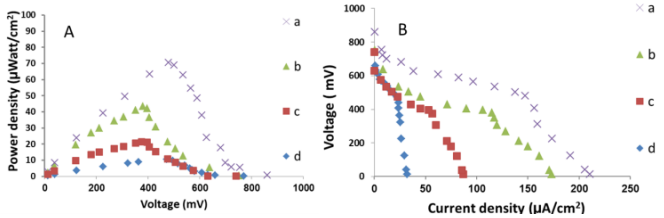

Fig. 4. Power outputs (A) and polarization curves (B) of BFCs constructed with (a) elongated ADHII-JK321/MB/MWCNTS/CPE anode, (b) normal ADHII-JK321/MB/MWCNTS/CPE anode, (c) Natural biofilm of *E. coli* covered CPE anode (d) and commercial ADHII enzyme on MWCNTS/CPE anode with free MB in solution. Measurements were performed under ambient temperature, in the presence of 1.5% (wt) ethanol. A potential of +700 mV vs Ag/AgCl was applied on the cathode.

$$f = Pmax\, Isc^{-1}\, Voc^{-1} \quad (1)$$

This result indicates that this anode has an effective electrical contact and a reduced loss in mass transport.

Conclusions

We have demonstrated a combination of several strategies including enzyme surface display, bacterial elongation and LbL assembly to create a hierarchically structured artificial biofilm based anode. This anode has shown improved mass transport, electrical contact, and bacteria-electrode communication. Biofuel cell assembled from this bioanode has shown a maximum power output of 70.6 µW/cm^2. It is not simple to compare the performance of this system to other ethanol dependent BFCs (either microbial or enzyme based) since we have used a potentiostatically controlled cathode, however, if the BFC is not limited by the cathode, the performance of the bioanode that was constructed in this study is superior over reported ethanol based MFCs which stresses further our hypothesis that an artificial conducting biofilm maybe beneficial in MFCs.

Acknowledgments

Research was supported by an Israel Science Foundation (ISF) Program (232/13), (L. A.) as well as by the PBC Program for Fellowships for outstanding post-doctoral researchers from China and India (L. X.). We are thankful to Prof. Tomas F. Meyer from Max Planck Institute for Infection Biology, Berlin for the generous contribution of E. coli strain JK321 as well as plasmid pJM7 harbouring the auto-display system. Technical assistance of Liron Amir, Orr Schlesinger, Jennifer Grushka, Alon Szczupak and Yonatan Chemla is greatly appreciated.

Notes and references

[a] *Department of Life Sciences and the Ilse Katz Institute for Nanoscale Science and Technology, P.O. Box 653, Beer-Sheva 84105, Israel. E-mail: alfontal@bgu.ac.il; Fax: +972 8 6479576; Tel: +972 8 6479066*
[b] *The Growing Base for State Key Laboratory, College of Chemical Science and Engineering, Qingdao University, Qingdao, Shandong 266071, China.*

† Electronic Supplementary Information (ESI) available: Detailed experimental procedures; control experiments related to ADHII activity investigation; comparison of electrochemical catalytic performance between different assembled anodes and calibration curves. See DOI: 10.1039/c000000x/

1. B. E. Logan, *Nat. Rev. Micro.*, 2009, **7**, 375-381.
2. B. E. Logan, B. Hamelers, R. Rozendal, U. Schröder, J. Keller, S. Freguia, P. Aelterman, W. Verstraete and K. Rabaey, *Environ. Sci. Technol.*, 2006, **40**, 5181-5192.
3. B. E. Logan, in *Microbial Fuel Cells*, John Wiley & Sons, Inc., 2008, pp. 1-11.
4. D. R. Lovley, Curr. Opin. Biotechnol., 2006, **17**, 327-332.
5. K. Bahartan, L. Amir, A. Israel, R. G. Lichtenstein and L. Alfonta, *ChemSusChem*, 2012, **5**, 1820-1825.
6. H. Liu, R. Ramnarayanan and B. E. Logan, *Environ. Sci. Technol.*, 2004, **38**, 2281-2285.
7. D. R. Bond, D. E. Holmes, L. M. Tender and D. R. Lovley, *Science*, 2002, **295**, 483-485.
8. C. Knight, K. Cavanagh, C. Munnings, T. Moore, K. Cheng and A. Kaksonen, in *Wireless Sensor Networks and Ecological Monitoring*, eds. S. C. Mukhopadhyay and J.-A. Jiang, Springer Berlin Heidelberg, 2013, vol. 3, pp. 151-178.
9. J. A. Cracknell, K. A. Vincent and F. A. Armstrong, *Chem. Rev.*, 2008, **108**, 2439-2461.
10. A. Szczupak, D. Kol-Kalman and L. Alfonta, *Chem. Commun.*, 2012, **48**, 49-51.
11. S. Fishilevich, L. Amir, Y. Fridman, A. Aharoni and L. Alfonta, *J. Am. Chem. Soc.*, 2009, **131**, 12052-12053.
12. L. Amir, S. A. Carnally, J. Rayo, S. Rosenne, S. Melamed Yerushalmi, O. Schlesinger, M. M. Meijler and L. Alfonta, *J. Am. Chem. Soc.*, 2012, **135**, 70-73.
13. L. Xia, B. Liang, L. Li, X. Tang, I. Palchetti, M. Mascini and A. Liu, *Biosens. Bioelectron.*, 2013, **44**, 160-163.
14. Y.-Y. Yu, H.-l. Chen, Y.-C. Yong, D.-H. Kim and H. Song, *Chem. Commun.*, 2011, **47**, 12825-12827.
15. E. Marsili, D. B. Baron, I. D. Shikhare, D. Coursolle, J. A. Gralnick and D. R. Bond, *Proc. Natl. Acad. Sci.*, 2008, **105**, 3968-3973.
16. Y. Yang, Y. Xiang, C. Xia, W.-M. Wu, G. Sun and M. Xu, *Bioresource. Technol.*, 2014, **164**, 270-275.
17. H.-S. Lee, C. I. Torres and B. E. Rittmann, *Environ. Sci. Technol.* 2009, **43**, 7571-7577.
18. C. Li, L. Zhang, L. Ding, H. Ren and H. Cui, *Biosens. Bioelectron.*, 2011, **26**, 4169-4176.
19. L. Peng, S.-J. You and J.-Y. Wang, *Biosens. Bioelectron.*, 2010, **25**, 1248-1251.
20. I. H. Park, M. Christy, P. Kim and K. S. Nahm, *Biosens. Bioelectron.*, 2014, **58**, 75-80.
21. F. Gao, L. Viry, M. Maugey, P. Poulin and N. Mano, *Nat. Commun.*, 2010, **1**.
22. A. Zebda, C. Gondran, A. Le Goff, M. Holzinger, P. Cinquin and S. Cosnier, *Nat. Commun.*, 2011, **2**, 370.
23. B. Rosenberg, L. Van Camp and T. Krigas, *Nature*, 1965, **205**, 698-699.
24. B. Rosenberg, E. Renshaw, L. Vancamp, J. Hartwick and J. Drobnik, *J. Bacteriol.*, 1967, **93**, 716-721.
25. S. A. Patil, K. Gorecki, C. Hagerhall and L. Gorton, *Energy. Environ. Sci.*, 2013, **6**, 2626-2630.
26. V. V. Chagovets, M. V. Kosevich, S. G. Stepanian, O. A. Boryak, V. S. Shelkovsky, V. V. Orlov, V. S. Leontiev, V. A. Pokrovskiy, L. Adamowicz and V. A. Karachevtsev, *J. Phys. Chem. C*, 2012, **116**, 20579-20590.
27. U. Schröder, J. Nießen and F. Scholz, *Angew. Chem. Int. Ed.*, 2003, **42**, 2880-2883.